Short Communication

For reprint orders, please contact reprints@futuremedicine.com

Regenerative Medicine

Novel hydrogel system eliminates subculturing and improves retention of nonsenescent mesenchymal stem cell populations

Jacob G Hodge[1,3], Jennifer L Robinson[1,2] & Adam J Mellott*[,3,4]
[1]Bioengineering Graduate Program, University of Kansas, Lawrence, KS 66045, USA
[2]Department of Chemical & Petroleum Engineering, University of Kansas, Lawrence, KS 66045, USA
[3]Department of Plastic Surgery, University of Kansas Medical Center, Kansas City, KS 66160, USA
[4]Ronawk, LLC, Olathe, KS 66062, USA
*Author for correspondence: Tel.: +1 913 588 8308; amellott@kumc.edu

Aim: To compare the physiological behavior of mesenchymal stem/stromal cells (MSCs) within an expandable tissue-mimetic 3D system relative to *in vitro* expansion in a traditional 2D system. **Methods:** Adipose-derived MSCs (ASCs) were continuously cultured for 6 weeks on either 2D culture plastic or in a 3D hydrogel system that eliminated subculturing. ASCs were assessed for senescence, 'stem-like' MSC markers, and ability for their secretome to augment a secondary cell population. **Results:** The 3D hydrogel system resulted in an enhanced retention of more regenerative, nonsenescent ASC populations that exhibited increased expression of 'stem-like' MSC surface markers. **Conclusion:** This study introduces a proof-of-concept design for a novel modular 3D system that can improve *in vitro* expansion of stem-like cell populations for future regenerative therapies.

Tweetable abstract: Novel tissue-mimetic 3D hydrogel system enhances the retention of nonsenescent ASC populations *in vitro* for up to 6 weeks in culture and eliminates the need to subculture, improving regenerative capacity of ASCs and their secreted biologics.

First draft submitted: 8 August 2022; Accepted for publication: 22 September 2022; Published online: 12 October 2022

Keywords: cell culture • hydrogels • regenerative medicine • stem cells • tissue engineering

Mesenchymal stem/stromal cells (MSCs) are a heterogeneous population of multipotent progenitor cells that are found in a variety of tissue sources within the human body, including bone marrow, dental pulp, umbilical cord and adipose tissue [1]. MSCs have earned a spotlight in the fields of tissue engineering and regenerative medicine for their intrinsically diverse regenerative and secretory properties [2]. The multipotent nature of MSCs originally garnered immense interest in the field of biomedical engineering due to the capacity for MSCs to differentiate into osteogenic, chondrogenic, adipogenic, nervous, skeletal and cardiac lineages to potentially form a neotissue or whole-organ replacement for diseased and damaged tissue within the body [1–3]. These types of therapies have often focused on the incorporation of MSCs with scaffolds and hydrogels of various complexities in order to control the differentiation of MSCs toward specific lineages.

Other MSC-based therapies that are currently being investigated include endovascular or direct injection of MSCs into locations of damaged tissue [2]. These therapies require further optimization due to cell death and radial diffusion of MSCs from the sites of injection, although ongoing research into delivery vehicles for MSC therapies such as scaffolds and hydrogel encapsulation have proven to be promising next steps in improving their efficiency and efficacy [4–9]. Similarly, another MSC-based therapy that has garnered interest involves the utilization of MSC-derived secretory products, called the secretome, as a form of acellular MSC therapy that circumvents some of the common limitations of cell-based therapies. MSCs' secreted byproducts include a heterogeneous variety of biomodulatory factors such as proteins, antioxidants, nucleic acids, exosomes and microvesicles, and have

Future Medicine

been shown to promote tissue regeneration and wound healing in a variety of applications [10–13]. Ultimately, for both cellular and acellular MSC-derived therapeutics, cells must be removed from a donor source and subsequently expanded *in vitro* to achieve sufficient cell numbers (often requiring anywhere from 10^7 to 10^9 MSCs at a minimum) to obtain a viable clinical product, which is associated with loss of a stem-like phenotype and often takes several weeks to achieve [14,15].

Traditionally, MSC *in vitro* expansion systems include the use of rigid, 2D plastic culture vessels to expand the cells as a monolayer and require multiple protease-dependent subculturing (passaging) events to achieve large enough cell quantities. Evidence suggests that traditional 2D culture systems are not ideal for stem cell expansion and can result in a loss of MSC multipotency, reduce viability, induce senescence and decrease secretion of regenerative factors [16–20]. Studies have demonstrated that stem cell differentiation and function are, in part, dependent on substrate mechanical properties [21,22], with more rigid substrates promoting osteogenic lineages and decreased viability, and softer substrates improving viability and the retention of 'stem-like' properties [21,23]. Thus, the decreased robustness of MSC populations seen in traditional 2D culture is likely due to a combination of the unphysiologically rigid substrate mechanics of 2D culture plastic, in addition to the overcrowding of cells in 2D monolayers and the need for continuous subculturing of cells. Ultimately, traditional 2D culture modalities likely result in less viable and more senescent cell populations over time, leading to impurities and/or an inconsistent secreted product that subsequently increases the variability between experimental assays and limits the potential downstream clinical benefits of MSC-derived therapies.

Early studies with 3D culture systems, including spheroid and organoid culture, have demonstrated their capacity to circumvent some of the limitations of 2D culture and improve the stem-like phenotype of MSC populations [24–26]. However, spheroid and organoid cultures are often limited in their size due to diffusional constraints and are prone to central regions of necrosis and cell death [27]. Additionally, spheroid/organoid culture can be labor-intensive and can require large and expensive bioreactor systems, such as stir-tank bioreactors, for long-term expansion applications that culminate in the need for artificial dissociation of the cellular clusters with proteases [24,28]. This process is especially true for industrial purposes with the goal of generating cellular or cellular-derived therapies. Moreover, a recent study investigating long-term culture of Wharton's jelly MSCs demonstrated an increased population of senescent cells after 3D spheroid culture [29]. Thus, the development of more efficient tissue-mimetic 3D culture systems that improve the long-term expansion of robust and stem-like cell populations are currently still under investigation. One promising approach is the utilization of 3D hydrogel cultures, due in part to the tailorability of the substrate composition and mechanics [30,31]. To date, many hydrogel systems have aimed to control differentiation and/or act as a delivery vehicle of stem cells, rather than to expand MSCs and maintain their stem-like properties [32–35]. Additionally, most current hydrogel formulations lack the porous microarchitecture that aids in cellular migration and nutrient diffusion.

In this study we set out to develop a proof of concept for a novel 3D hydrogel system that improves expansion outcomes of MSC populations, such as adipose-derived MSCs (ASCs). The customizable 3D hydrogel system is bioprinted and was formulated to be a bioinert substrate that closely mimicked native adipose tissue mechanics (Supplementary Figure 1) and ultimately acts like a tailored bioreactor for MSC expansion and collection of biologics. The 3D hydrogel system was constructed with a unique 'puzzle-piece' macrostructure design that enables easy addition of supplementary hydrogels. Additionally, the unique porous microarchitectural design permits mass transport and promotes cellular migration and proliferation, eliminating the need to subculture cells via cellular migration between hydrogels within the microchannels. The initial utilization of a bioinert substrate allowed for the investigation and observation of the potential role of the mechanical and dimensional properties of the 3D system on ASC senescence and stem-like phenotypic properties without introducing a bioactive substrate. We hypothesized that the softer, 3D hydrogel substrate would provide a more natural mechanical environment for the ASCs and result in the retention of nonsenescent stem-like ASC populations, relative to traditional 2D culture methodologies. Moreover, the unique architectural design would allow for continuous expansion of ASCs via cellular migration between the attached hydrogels, thus eliminating exposure of cells to negative 2D subculturing procedures and subsequent sequelae.

Materials & methods

Cell culture

Human ASCs (Lot #18TL212639, 23-year-old female, Black), human keratinocytes (KCs; Lot #18TL318559, 62-year-old male, Caucasian) obtained from Lonza (Basel, Switzerland) were utilized for this study. MSC-GM

Mesenchymal Stem Cell Growth Medium BulletKit™ was obtained from Lonza (#PT-3001) and used for ASCs. MesenCult™-ACF Plus Medium Kit (Stem Cell Technologies, BC, Canada; Cat. #05445) was used as the serum-free medium. DermaLife K Keratinocyte Medium Complete Kit was obtained from Lifeline Cell Technologies (MD, USA; #LL-0007) and used for KCs.

3D-printed hydrogel cell culture system

The bioinert 3D hydrogel system is approximately 1 × 1 × 1 cm and is a polyethylene glycol (PEG)-based system called a Tissue-Block (T-Block; Ronawk, KS, USA) which contains a unique microarchitectural design and was fabricated to resemble the mechanics of native adipose soft tissue (Supplementary Figure 1) and demonstrated no significant changes in mechanical properties over 3 months. The 3D hydrogels were placed into a glass six-well culture plate for culturing. Fibronectin is a commonly selected coating substrate for ASCs due to their natural secretion of fibronectin. Because the cells do not efficiently adhere/attach to the PEG-based polymer, both the 2D culture plastic/glass and 3D hydrogel were coated with fibronectin at a concentration of 5 μg/cm^2 to enhance the initial cell attachment. The concentration of fibronectin was standardized to surface area due to the inherent surface-area-to-volume differences between 2D and 3D systems. The approximate surface area of the 3D hydrogel was calculated from the 3D model used for bioprinting.

Expansion of ASCs & KCs

ASCs and KCs were seeded within a T-150 flask and cultured until ~80% confluence before subculturing (passaging). Subculturing of cells was performed by removing culture media, washing thrice with Hanks' balanced salt solution (HBSS, MA, USA; calcium-free, magnesium-free) and incubating with 0.05% Trypsin/EDTA (Lonza; Cat. #CC-3232) at 37°C for 5 min. Trypsin was neutralized with serum and the cells were centrifuged at 500 × g for 5 min, then pelleted and resuspended for reseeding on new 2D tissue culture plastic vessels. ASCs at passage 1 (P1) were reseeded onto 2D culture plastic or onto/within the bioprinted 3D hydrogel system via dropwise addition of a concentrated cell solution to the surface of the hydrogels. This process was repeated with the residual cell solution five times to ensure efficient cell seeding. This repetitive seeding process allowed for the cells to distribute throughout the microporous structure within the hydrogel system. Given that the increased surface area and attachment of additional hydrogels eliminated the need for subculturing for this study, a passage-equivalence time point was utilized to allow for analogous comparison with 2D culture. Thus, a passaging event typically occurred every 4–5 days in 2D culture for ASCs but not in 3D culture. After 4–5 days of 2D culture for P2 ASCs, the cells were then subcultured and considered to be P3 in 2D, and the 3D ASCs were then considered P3 passage-equivalent. Culture expansion was determined based on the known 2D and 3D surface areas, initial cell seeding density and average population doubling time of 2.25 days (experimentally determined in 2D; data not shown) for the ASCs in order to standardize cell numbers. ASCs were seeded at a standardized concentration of 5000 cells/cm^2 for assays. Media supplementation was standardized to 150 μl/cm^2 for ASC expansion to account for dilutional differences in surface-area-to-volume ratio between 2D and 3D culture.

ASC phenotype characterization

The MSC stem-like phenotype was evaluated for the ASCs at P1/2/6/10 via immunolabel characterization of three key MSC surface markers (CD73/90/105). ASCs were either continuously subcultured in a T-150 flask or allowed to expand within the 3D hydrogel system. At each respective passage time point, cells were seeded in 2D at a standardized density of ~5000 cells/cm^2 onto a 96-well glass culture plate (Cellvis, CA, USA; Cat. #P96-1.5H-N) for 2 days, fixed, then assessed for ASC phenotype via immunolabeling for surface CD markers. For ASCs within the 3D culture system, cells were fixed and stained *in situ*. Positive staining for CD73/90/105 and negative staining for CD34/45 was used to denote a stem-like MSC phenotype for this study. After fixation with 4% paraformaldehyde, cells were washed thrice with HBSS and placed in blocking buffer (1% donkey serum in HBSS) for 1 h. After blocking, primary antibodies for CD73 (Abcam, MA, USA; Cat. #133582; 1:100), CD90 (Abcam; Cat. #181469; 1:100), CD105 (Abcam; Cat. #231774; 1:100), CD34 (Abcam; Cat. #81289; 1:200) or CD45 (Abcam; Cat. #40763; 1:200) were added and the cells incubated overnight at 4°C. The next day cells were washed thrice and secondary antibodies were applied for 1 h, followed by three additional washes. Cells were counterstained with Hoechst 33342 (Invitrogen, MA, USA; Cat. #H3570; 1:1000) and Alexa Fluor® 647 Phalloidin (Invitrogen; Cat. #A22287; 1:1000). Immunofluorescence was assessed with a Revolve microscope using filters for 4′,6-diamidino-2-phenylindole (DAPI; EX-380/30, EM-450/50), fluorescein isothiocyanate (EX-470/40, EM-525/50); Texas Red

(EX-560/40, EM-630/75) and Cy5 (EX-630/40, EM-700/75) (Echo, CA, USA) and 20× objective (Olympus, Tokyo, Japan; UPlanSApo, 0.75NA). ASC stem-like phenotypic quantification was carried out in quadruplicate (n = 4), with images taken from a total of ten random fields of view per biological replicate (2D = per well; 3D = per hydrogel), to achieve up to 40 total measured values for each sample. Total nuclei were counted, and total positive cells were evaluated. Phalloidin counterstain was used to aid in localization of positive staining. ASCs characterized at P1 were used as a baseline for comparison (Supplementary Figure 2).

ASC senescence characterization

Similar to the ASC phenotyping methodology above, assessment of ASC senescence was performed. ASCs were continuously subcultured in a T-150 culture flask until each respective assay time point, when they were seeded onto a 96-well glass culture plate. ASCs in the 96-well plate were allowed to acclimate in serum-based media for 2 days, fixed, then assessed for senescent activity via immunofluorescent labeling of β-galactosidase activity with the CellEvent™ Senescence Green Detection Kit (Invitrogen; Cat. #C10850), per manufacturer's instructions. ASCs in the 3D system were assessed simultaneously at the P2/6/10 passage-equivalent time points. Similar to the method above, cells were counterstained with Hoechst and Phalloidin. Senescence characterization was carried out in quadruplicate (n = 4), with images taken from a total of ten random fields of view per biological replicate, to achieve up to 40 total measured values per sample. Total nuclei were counted, and total senescent positive and negative cells were determined.

Isolation of ASC-conditioned media

Media supplementation was standardized for ASC expansion to account for dilutional differences in surface-area-to-volume ratio between 2D and 3D cultures. Media were changed every 2 days. For ASC-conditioned medium (ASC-CM) collection, MSC-GM was removed and cells were washed with HBSS thrice, then cultured with serum-free MSC media for 48 h before collection (for both 2D and 3D cultures). Collected ASC-CM was then centrifuged at 1500 × g for 10 min to eliminate cell debris, Steriflip-filtered with a 0.22-μm filter and stored at -80°C until use.

KC activity after ASC-CM treatment

ASC-CM was collected at each respective time point per the protocol above. ASC-CM was then placed on KCs for up to 24 h to assess its capacity to modulate metabolic, proliferative or migratory activity to evaluate wound healing capabilities of the ASC-CM. For these studies, ASC-CM was added at a 1:1 ratio with KC growth medium. Experimental assays were performed per the manufacturer's instructions. PrestoBlue fluorescence was obtained at 560/590 nm (n = 4) and used for evaluation of metabolic activity after 24 h of ASC-CM treatment. Hoechst was added to PrestoBlue samples and values were displayed as average relative fluorescence unit values of PrestoBlue/Hoechst signal in order to control for potential differences in cell numbers and obtain approximate metabolic activity per cell. PicoGreen fluorescence was obtained at 485/535 nm (n = 4) and used for evaluation of cell number as a surrogate measurement of KC proliferation after 24 h of ASC-CM culture. Total cell numbers per 96-well plate were calculated based on an average DNA content of 7.7 pg/cell. KC scratch assays were performed to evaluate changes in wound size as a surrogate measurement of KC migration (n = 3). Migration images were taken using an ImageXpress Micro XLS Imaging System (Molecular Devices, CA, USA). The entire wound was imaged for each wound triplicate and three different wound regions per wound triplicate were used to calculate wound area. The three wound area values were averaged per triplicate and per time point for each group and displayed as percentage wound area recovered (n = 3).

Statistical analysis

All data are reported as means with standard error of the mean. Characterization analyses of ASC populations with immunolabeling for senescence and CD markers were evaluated with a two-way analysis of variance. KC metabolic, proliferative and migratory activities were evaluated with a two-way analysis of variance. Data were tested for normality via Shapiro–Wilk and Kolmogorov–Smirnov tests and plotted with a QQ plot. GraphPad Prism 9.0.2 software (GraphPad, CA, USA) was used for the analyses, and a p-value < 0.05 was considered significant.

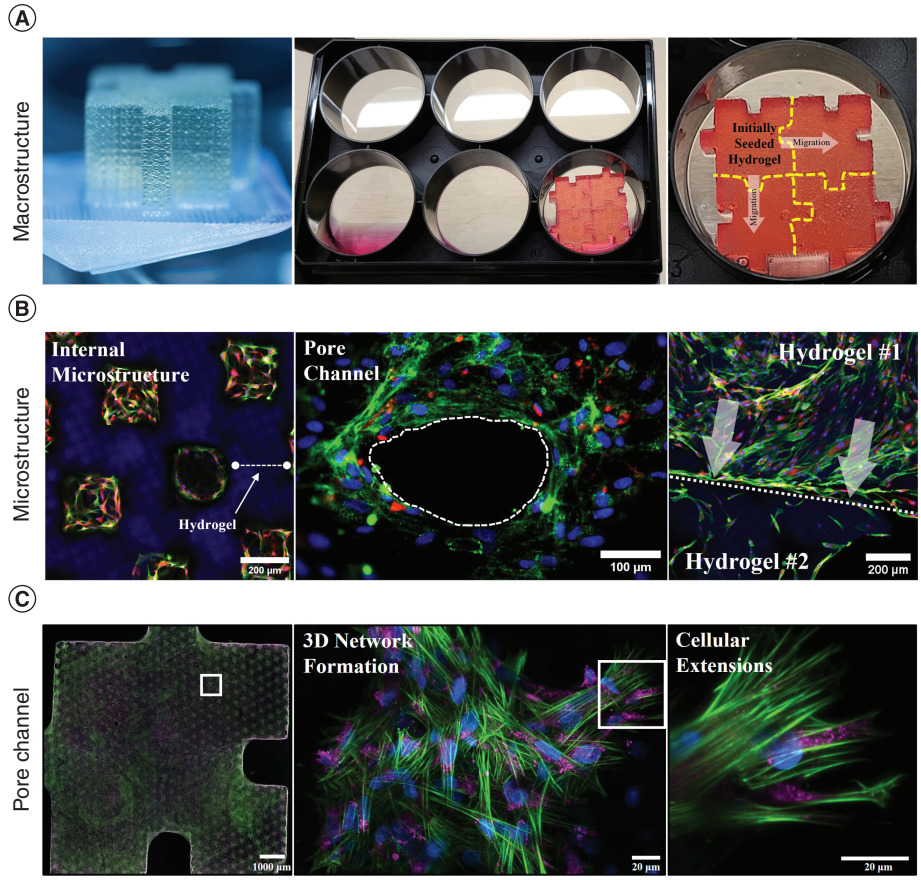

Figure 1. Unique 3D hydrogel design eliminates subculturing. (A) Depictions of the macrostructure of the hydrogel system. (Left) A single photographic image of the ~1-cm^3 3D hydrogel system. (Middle) A photographic image of four hydrogels connected to each other within a six-well plate. (Right) A photographic image of four hydrogels, connected with annotations depicting the migration of cells out/from an initially seeded hydrogel into/toward supplementally attached hydrogels without cells. **(B)** Depictions of the microstructure of the hydrogel system. (Left) Confocal microscopy image of a cross-section of the internal structure of the hydrogel depicting ASCs migrating and proliferating within the porous architecture. The small white arrow indicates polymeric struts of the hydrogel. Blue = Hoechst; green = phalloidin; red = Mitotracker. (Middle) Fluorescent image of ASCs lining an individual pore within the microstructure of the hydrogel system. Blue = Hoechst; green = wheat germ agglutinin; Red = Mitotracker. (Right) Confocal microscopy z-stack image of ASC migrating from an initially seeded hydrogel (Hydrogel #1) into a newly attached hydrogel (Hydrogel #2). Large white arrows indicate directionality of ASC migration; white dashed line indicates the junction of the two attached hydrogels. **(C)** Three images depicting a 3D z-stack of images within a single pore channel to highlight (middle) the 3D networks formed by ASCs and (right) cellular extension protruding from the cells. (Left) Low-magnification image of the entire stained hydrogel. Images in **(C)** were acquired by Nikon on their AXR Confocal Imaging System. Blue = Hoechst; Green = phalloidin; Pink = Mitotracker.
ASC: Adipose-derived mesenchymal stem/stromal cell.

Results

Unique 3D hydrogel design eliminates subculturing

The ~1-cm^3 3D-printed hydrogel system contains a unique 'puzzle-piece' macrostructure that allows the continuous addition of supplementary hydrogels (Figure 1A) and promotes the migration of cells from the primary seeded hydrogel into the newly attached hydrogels (Figure 1A & B). ASCs were cultured within/onto a single hydrogel system for 2 weeks and allowed to migrate throughout the hydrogel. Subsequently, an additional hydrogel was added for 5 days, and cells were allowed to migrate to the newly attached hydrogel. The cells were then stained and assessed for migration and proliferation between the two hydrogels (Figure 1B). ASCs were seen lining the porous channels beyond the superficial surface within the internal structure and can be seen forming networks within the hydrogel pores (Figure 1B & C). Cells were able to migrate both across the surface of attached hydrogels and within the microchannels, and can be seen with numerous cellular extensions and focal adhesions protruding from the

cells to aid in migration (Figure 1C). The interaction of ASCs in 3D and the formation of 3D networks within the hydrogel microarchitecture are further highlighted in Supplementary Videos 1 & 2. Notably, ASCs can be seen lining the surface of the hydrogel and migrating down into one of the pore channels, ultimately interacting in three dimensions with other cell populations within the pore.

Retention of stem-like MSC surface markers in 3D hydrogel over time

Evaluation of stem-like ASC populations over time was performed via immunolabeling quantification of the CD markers CD73/90/105 (Figure 2A). The prevalence of stem-like CD markers declined over time in both 2D and 3D systems; however, 2D culture had a significantly enhanced rate of loss of these markers relative to the 3D system (Figure 2B). Similarly, there was an apparent decrease in intensity of positively stained cells over time in both 2D and 3D systems. Culture within the 3D system resulted in a significant retention at all passage time points for all three positive stem-like markers, except for the initial P2 comparison of CD105. The significant loss of a stem-like phenotype in 2D culture can be seen clearly when comparing ASCs in 3D at P6 and P10 versus ASCs in 2D at P2 (Figure 2B). Over the course of five or nine passage equivalents in 3D (i.e., 3 or 6 weeks in the 3D system for P6 or P10, respectively) and only one passage event in 2D (seeded at P1), the ASCs had similar expression patterns for multiple CD markers, with only a significant difference between 3D expression of CD105 at P10 relative to 2D CD105 at P2 (Figure 2B). Both systems maintained a low population (<5%) of positive-staining cells for CD34 and CD45 markers.

Delayed induction of senescence in 3D hydrogel over time

The prevalence of senescent ASC populations over time was evaluated via fluorescent labeling of β-galactosidase activity, a commonly utilized surrogate measurement of cellular senescence (Figure 3A). The baseline expression of β-galactosidase activity was ~5% for both 2D and 3D ASCs at P2. Over the course of multiple passaging events in 2D, senescence was significantly increased in 2D, with 11.7 and 22.5% senescent cells at P6 and P10, respectively (Figure 3B). Conversely, in the 3D system there was no significant change in the prevalence of senescence over time in ASC populations for the time course of this study (6 weeks) (Figure 3B). Similarly, there were notable differences in cellular morphology in the 2D system versus the 3D system. More specifically, 2D ASCs appear to be more flattened, with a more heterogeneous morphological distribution and an apparent increase in cell size over time in culture, whereas the 3D ASCs maintained a more homogeneous morphology with no observable change in cell size or morphology.

Retention of ASC conditioned media wound healing capacity

Evaluation of the ASC-CM's functional capacity to modulate a secondary cell population was utilized to demonstrate the dynamic interrelationship between ASC population phenotype and ability to promote wound healing activity in KCs (Figure 4D). KCs were treated with either 2D or 3D ASC-CM from each respective time point for up to 24 h. KCs treated with ASC-CM from 2D cultures showed a significant drop in recovered wound area when treated with P6 and P10 ASC-CM, relative to P2. There was also a slight decrease noted in KC migratory activity observed with 3D ASC-CM from P10 relative to P2 (Figure 4A & B). Overall, 3D ASC-CM maintained a significantly higher ability to enhance KC migration and close their respective wounds, relative to their 2D ASC-CM counterparts. The metabolic activity of KCs demonstrated a decreasing trend when treated with ASC-CM from 2D-expanded cells, with a significant decrease noted in P10 relative to P2 ASC-CM (Figure 4C). No significant differences were observed with ASC-CM from 3D cultures over time. Similarly, the proliferative activity of KCs treated with ASC-CM from 2D cultures demonstrated a decreasing trend, with a significant difference between P10 and P2 ASC-CM, but no significant change noted when KCs were treated with ASC-CM from 3D cultures (Figure 4D). Moreover, the proliferative activity of KCs treated with 3D ASC-CM from P6 and P10 was significantly higher than that of their 2D ASC-CM counterparts.

Discussion

The inherent regenerative properties of MSCs have garnered immense interest for advancing the field of regenerative medicine and tissue engineering. However, MSCs typically must first be removed from a donor tissue source and cultured outside the body within an artificial environment not native to human tissue. To date, commercially available *in vitro* expansion systems are almost exclusively 2D in nature. Rigid 2D systems are unphysiological for the cells and rapidly result in the loss of MSC multipotent stem-like features, with subsequent loss of viability and

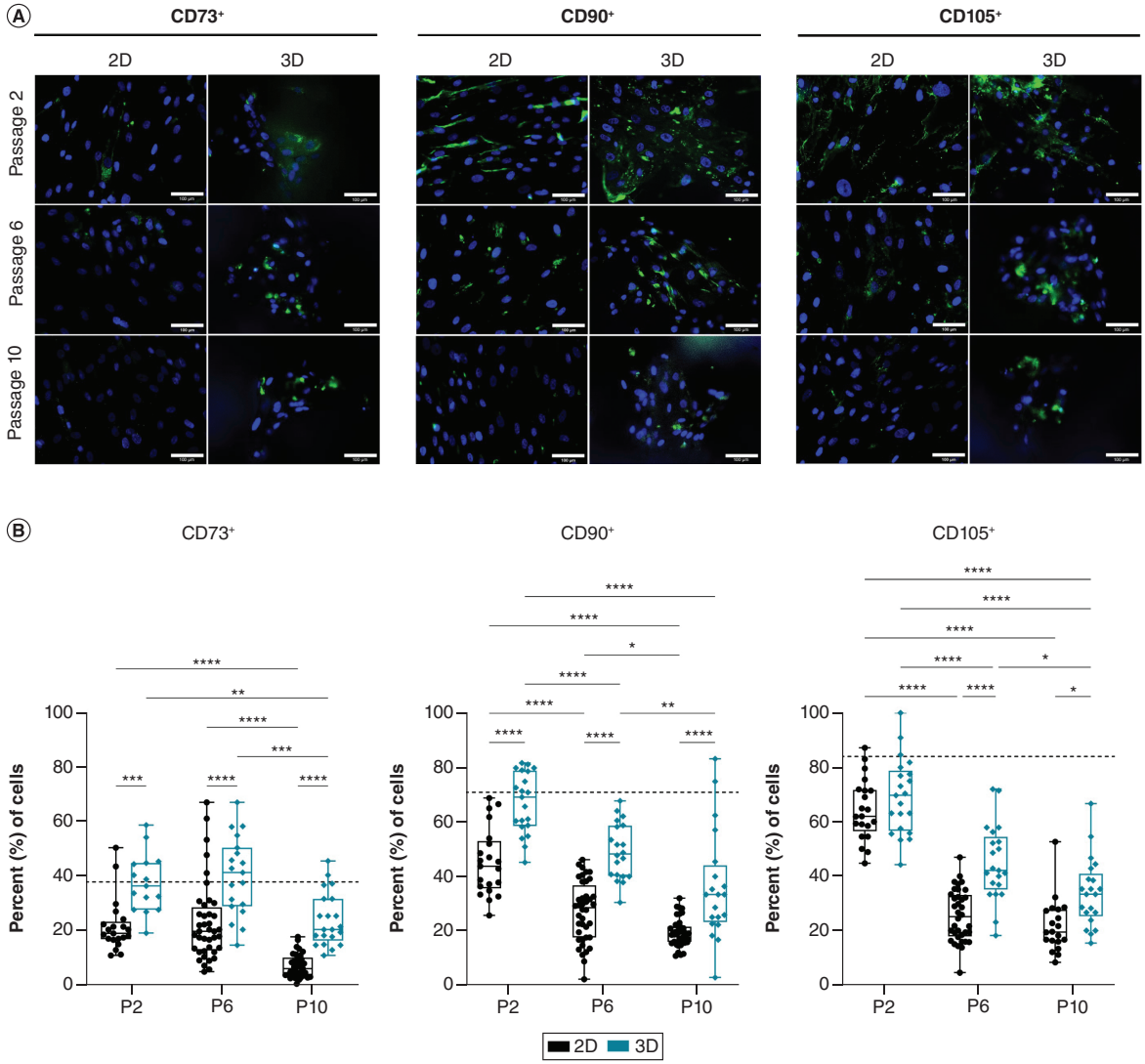

Figure 2. Retention of stem-like surface markers in 3D hydrogel over time. Adipose-derived mesenchymal stem/stromal cells (ASCs) were seeded at passage 1 (P1) within the 3D hydrogel system or traditional 2D culture. ASCs were continuously subcultured and assessed at P2, P6 and P10 for 2D culture. The ASCs in the 3D hydrogel system were compared with their respective 2D counterparts via passage-equivalent time points. Three additional hydrogels were added to each individual hydrogel at the 2-week mark and left for the remainder of the culture period to provide adequate surface area for continuous cell growth. **(A)** At each respective time point (P2, P6 and P10), representative images of 2D (leftmost columns) and 3D (right-most columns) cultured ASCs stained for either CD73 (left), CD90 (middle) or CD105 (right) are depicted. CD marker staining is denoted by green in the images. Samples were counterstained with Hoechst (blue) and phalloidin (not shown). **(B)** Quantification of imaging data was performed and total percentage of positive cells denoted by box-and-whiskers plots for each marker. Each individual point indicates quantification of a single image of ASCs in 2D (black circles) or 3D (teal diamonds) cultures using a 20× objective. Samples were analyzed in quadruplicate (n = 4). Scale bar = 100 μm. Error bars are standard error of the mean.
*$p < 0.05$; **$p < 0.01$; ***$p < 0.001$; ****$p < 0.0001$.

induction of senescence [16,18,36]. These changes lead to MSC populations with significantly reduced regenerative capabilities, which is compounded by a lack of standardized cell culture conditions, creating a significant bottleneck in the growth and development of regenerative therapeutics. Thus, there is a critical need to develop culture systems for MSC expansion that are 3D and more tissue-mimetic in their mechanical, architectural and substrate composition properties and which can ultimately circumvent many of the limitations of traditional 2D culture, such as the continuous need for subculturing.

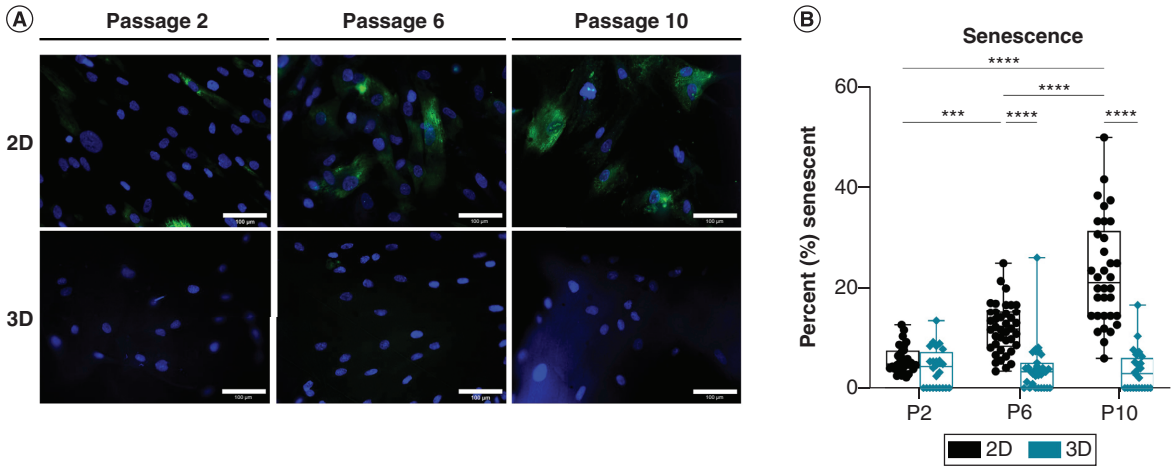

Figure 3. Delayed induction of senescence in 3D hydrogel over time. Adipose-derived mesenchymal stem/stromal cells (ASCs) were seeded at passage 1 (P1) within the 3D hydrogel system or traditional 2D culture. ASCs were continuously subcultured and assessed at P2, P6 and P10 for 2D culture. The ASCs in the 3D hydrogel system were compared with their respective 2D counterparts via passage-equivalent time points. Three additional hydrogels were added to each individual hydrogel at the 2-week mark and left for the remainder of the culture period to provide adequate surface area for continuous cell growth. **(A)** At each respective time point (P2, P6 and P10), representative images of 2D (top row) and 3D (bottom row) cultured ASCs stained for β-galactosidase (green) are depicted. Samples were counterstained with Hoechst (blue) and phalloidin (not shown). **(B)** Quantification of imaging data was performed and total percentage of positive cells denoted by box-and-whiskers plots for each marker. Each individual point indicates quantification of a single image of ASCs in 2D (black circles) or 3D (teal diamonds) using a 20× objective. Samples were analyzed in quadruplicate (n = 4). Scale bar = 100 μm. Error bars are standard error of the mean.
***$p < 0.001$; ****$p < 0.0001$.

Recent advancements in 3D systems have demonstrated progress toward producing MSC populations that are more stem-like. However, 3D systems such as spheroids, organoids, microspheres and many scaffold systems typically do not closely mimic the native mechanics of their cell/tissue source (e.g., adipose mechanics for ASCs) and often require large bioreactor systems and continuous subculturing to achieve large-scale cell numbers for clinical use. However, tissue-engineered hydrogel systems appear to be advantageous toward producing tailorable, tissue-mimetic systems for cell culture systems [30,31]. More specifically, the mechanotransductive response to the softer substrate of hydrogels is thought to aid in the retention of stem-like characteristics [23,37,38]. Unfortunately, most current hydrogel systems are manufactured to promote controlled differentiation of stem cells toward a specific tissue lineage and not to allow the cells to maintain a stem-like phenotype for long-term expansion [34,39–44]. Ultimately, an ideal MSC hydrogel expansion system would protect against senescence, while also improving the retention of a regenerative stem-like phenotype and permitting long-term expansion with minimal subculturing or user intervention.

Although MSC-based therapies have demonstrated promise, with over 1000 clinical trials to date listed with the US FDA, they have not advanced as quickly as previously thought. This is considered to be due, at least in part, to the detrimental impact senescent MSC populations may have on tissue regeneration [45,46]. Senescence is a progressive form of cell-cycle arrest, typically due to DNA and/or oxidative damage, which results in MSCs with impaired DNA-repair modalities that no longer proliferate and exhibit a loss of multipotency [47–49]. Moreover, senescent MSCs have been shown to secrete factors that negatively impact tissue regeneration and wound healing by impairing angiogenesis, increasing oxidative stress and exacerbating inflammation via the secretion of factors known as the senescence-associated secretory phenotype [50–52]. The composition of this phenotype can be heterogeneous and is dependent on the mechanism of senescence induction and environmental stimuli; therefore, this likely contributes to the heterogeneity in patient outcomes seen in clinical trials with both cell-based and acellular therapies [53–55]. Thus, developing an *in vitro* culture expansion system that limits/prevents the induction of senescence in healthy allogeneic or autologous MSC populations intended for patients would improve the efficacy and consistency of MSC-based clinical therapies.

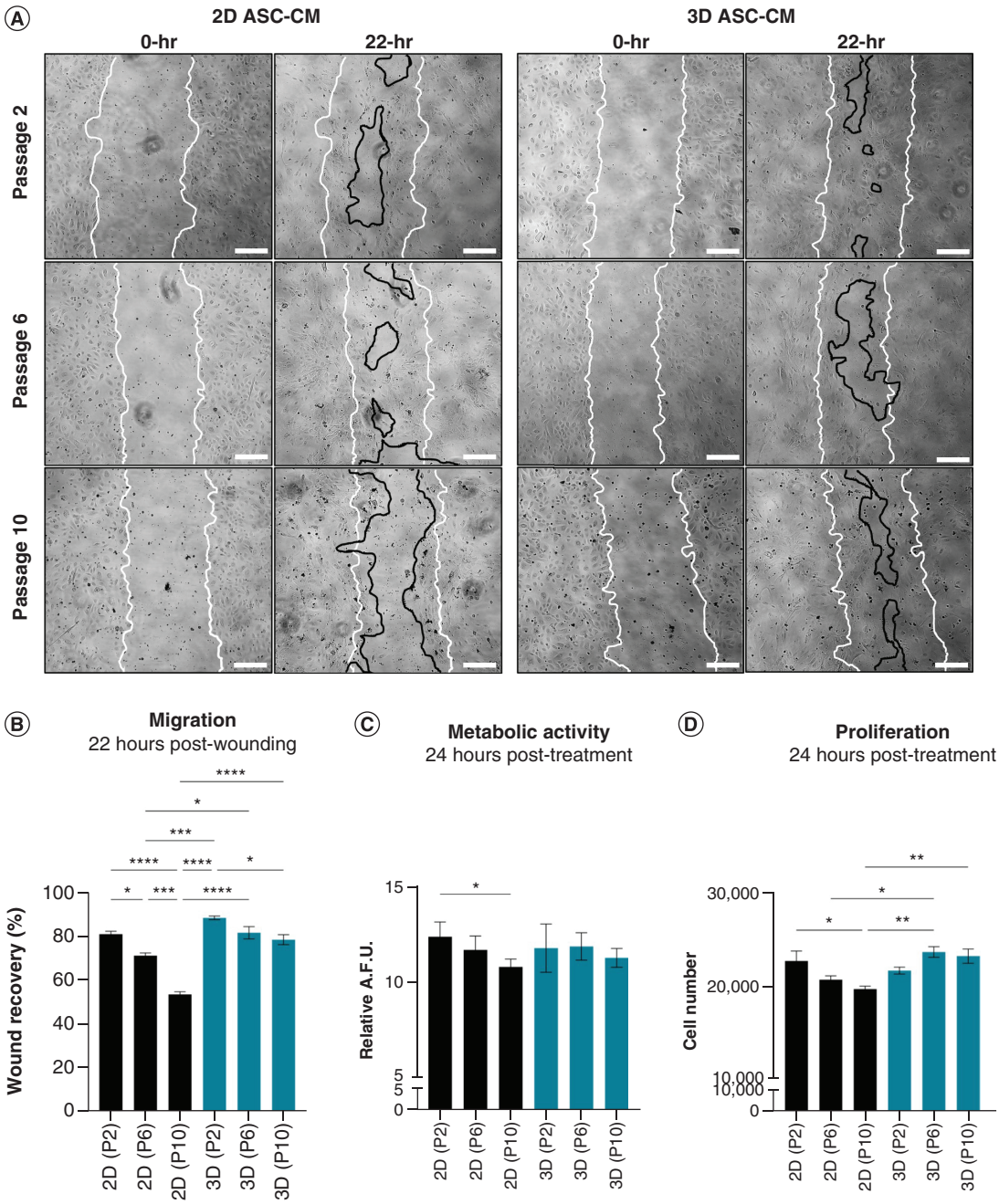

Figure 4. Retention of wound healing capacity in adipose-derived mesenchymal stem/stromal cell-conditioned media. ASC-CM from 2D and 3D from each respective time point was used to treat keratinocytes, which were then assessed for changes in their migratory, metabolic and proliferative activity. **(A & B)** Migratory activity was assessed via a scratch assay. **(A)** Whole-well image scans were acquired, and representative images of the wound images are provided. White solid lines denote original wound boundaries. Black solid lines outline the remaining wound area. **(B)** The average wound area after 22 h was determined and performed in triplicate. **(C)** Metabolic activity was quantified via PrestoBlue and is displayed as an average value of relative fluorescent units. **(D)** Proliferative activity was quantified via PicoGreen and the average cell number was determined. Keratinocytes treated with 2D ASC-CM are denoted with black bars; keratinocytes treated with 3D ASC-CM are denoted with teal bars. Scale bar = 500 μm. *$p < 0.05$; **$p < 0.01$; ***$p < 0.001$; ****$p < 0.0001$. Error bars are standard error of the mean.
ASC: Adipose-derived mesenchymal stem/stromal cell.

In this proof-of-concept study, culture of ASCs within a traditional 2D culture system resulted in a significant increase in senescence, as previously established in literature. Conversely, the 3D hydrogel system resulted in no significant changes of senescence in ASC populations over the course of the 6-week study (i.e., 10 passage equivalents). Moreover, changes in cell morphology and size can be indicative of phenotypic changes; the apparent increase in cell size seen in the 2D ASCs may be associated with the induction of senescence and thus further supports the β-galactosidase imaging data and prior literature. Overall, these data support the previous hypothesis that 3D culture and substrate mechanics maintain a protective role against senescence. However, with our 3D hydrogel system the need for subculturing is eliminated, and secreted by-products are more readily accessible versus more traditional poured/molded hydrogels that lack a porous microarchitecture. Further studies will be needed to assess potential dynamic mechanisms at play (e.g., induction of telomerase, protection against oxidative damage or increased DNA repair mechanisms) to establish the protective role of 3D culture seen in this study. Moreover, evaluating what the inciting events are that drive the progression toward *in vitro* senescence, and whether they can be circumvented with appropriate culture systems, requires further investigation. This study offers insight into future design considerations for improving 3D cell culture modalities for MSC expansion.

Similarly, the stem-like phenotype of MSCs is critical to their regenerative potential and can rapidly change depending on the culture environment of the cells. MSC populations that differentiate and lose their stem-like characteristics result in variability of cellular phenotype and alterations in secretome composition, ultimately decreasing the consistency of regenerative MSC therapeutics, both cellular and acellular. Thus, MSC populations such as ASCs are often used within only a few passaging events in an attempt to circumvent the loss of regenerative potential. However, as we see in this study, even within one additional passaging event in 2D culture, ASCs significantly alter their expression of stem-like markers. Moreover, ASCs expanded in 3D culture for six or ten passaging equivalents (i.e., P6 or P10) over 6 weeks maintained similar expression levels of several markers relative to the baseline P2 ASCs, and a higher expression relative to their respective 2D counterparts, further highlighting the detrimental effects of 2D culture systems on MSC populations and the potential protective effects of 3D culture. The ability to improve the retention of stem-like properties within MSC populations for longer periods of time is desirable for a multitude of applications, including cell therapies, regenerative tissue engineering, immunotherapy and production of secreted biologics.

As previously mentioned, recent MSC therapies have expanded into investigating biologics as a potential regenerative therapy. MSC populations are highly adaptive in nature, and are known to sense their surrounding environmental stimuli and secrete factors accordingly. Thus, secreted bioactive compounds act to coordinate and bridge a variety of tissue reparative processes in an autocrine, paracrine or endocrine manner. In this study, the conditioned media from ASCs cultured in 2D versus the 3D system were collected over time and utilized as a therapeutic for a secondary cell population, KCs, as a means to functionally assess the phenotype of the ASC secretome toward promoting wound healing activity. Working under the hypothesis that the ASC phenotype deteriorates over time in 2D cultures but is sustained in the 3D system, we expected to see a gradual decline in regenerative capabilities of the ASC-CM from 2D cultures but minimal changes in ASC-CM from 3D cultures. This hypothesis was supported by the metabolic, proliferative and migratory data of KCs treated with ASC-CM. ASC-CM from 2D cultures demonstrated a steady decline in ability to augment KC activity and was consistently outperformed by its 3D counterpart over the course of the study. To our knowledge, this is the first direct comparison of ASC phenotypic changes over time in 2D and 3D cultures, and the first examination of how those changes potentially correlate to the regenerative wound healing capacity of the ASC secretome on KC functionality.

The limitations of this study include the formulation of the hydrogel system being intentionally bioinert in order to eliminate any contribution of a bioactive substrate, and thus it was not degradable. As a result, adequate removal of cells from this formulation was not feasible. Therefore, we utilized immunofluorescent labeling as an alternative to flow cytometry or RNA analysis to demonstrate senescence and phenotype of MSC populations. However, the ability to perform *in situ* visualization of an adherent population such as MSCs without the need to resuspend them is an advantage of immunolabeling over cytometry. Moreover, the relative comparison between 2D and 3D cultures, paired with the functional data of the ASC-CM, helps provide a supportive and holistic perspective that reinforces the immunolabeling data, although a more comprehensive analysis of the secretome is needed to assess both qualitative and quantitative changes. Future hydrogel formulations will aim to be biodegradable, such as insertion of enzyme-sensitive sequences or utilization of native matrix-derived compounds, while also incorporating the advantages and design of this proof-of-concept system, including the mechanics, modularity, architecture and

elimination of subculturing. Lastly, follow-up studies to directly compare the performance of this 3D hydrogel system versus other 3D systems will provide a better understanding of the relative benefits of this new system.

Conclusion

In this study we introduce the proof-of-concept of a novel 3D hydrogel system to demonstrate the benefits of culturing MSCs in a system that more closely resembles their native tissue mechanics. Our 3D system contains a unique architectural design that does not impede effective mass and fluid transport while also allowing the movement of cells within and between attached hydrogels, in effect providing a continuous 3D culture system that eliminates the need to subculture cells. The continuity is achieved by the addition of supplemental hydrogels to previously seeded hydrogels, much like attaching together two puzzle pieces. The porous microarchitecture creates a 'tunneling' system for the cells to interact in the x-, y- and z- planes and to migrate within and between hydrogels, in addition to surface migration at attachment points. This is the first demonstration of such a system, to our knowledge. The results of this study provide a framework for future studies; specifically, after establishing the beneficial effects of this bioinert 3D hydrogel system on ASC populations, future studies will aim to further tailor the 3D system's tissue-mimetic properties and control the regenerative activity of MSCs. Together, these data demonstrate the potential of a novel 3D culture system to enhance and retain the overall regenerative capacity of MSC populations over time, with the added benefit of further improving the regenerative and wound healing capabilities of MSC-derived biologics for a variety of tissue reparative applications.

Summary points

- Mesenchymal stem/stromal cell (MSC) populations are highly adaptable progenitor cell populations that contain inherent regenerative capabilities due to their multipotent and secretory nature.
- MSC-secreted by-products, also known as the secretome, contain a heterogeneous milieu of biomodulatory factors such as proteins, antioxidants, nucleic acids, exosomes and microvesicles. The secretome composition is dependent on MSCs' adaptive responses and environmental cues.
- The acellular MSC secretome has the ability to directly modulate tissue engineering and wound healing processes independent of MSC cellular feedback.
- In order to achieve enough MSCs for a clinical product, MSCs must be explanted from the body and expanded within an artificial environment not native to human tissue.
- To date, most commercially available *in vitro* expansion systems are 2D in nature, forcing MSCs to grow in a 2D monolayer. These rigid 2D systems are unphysiological and result in senescence, loss of MSC multipotency, and impaired secretory activity.
- Traditional 2D culture systems result in impurities and/or an inconsistent secretory and cellular product due to less consistent and viable MSC populations within 2D culture systems.
- Senescent MSCs have been shown to secrete factors that negatively impact tissue regeneration and wound healing.
- Recent advancements in 3D systems have demonstrated progress toward producing MSC populations that are able to maintain their stem-like characteristics for an extended period of time. However, most current 3D culture expansion systems still do not mimic native tissue mechanics for the MSC cell/tissue source.
- Tissue-engineered hydrogel systems offer many advantages for producing tailorable, tissue-mimetic systems for cell culture.
- Most current 3D hydrogel systems lack an inherent porous microarchitecture, are used as delivery vehicles and/or are manufactured to control and promote specific differentiation activity of MSC populations.
- Our novel 3D hydrogel system contains a unique architectural design that does not impede effective mass and fluid transport, permits the movement of cells within and between attached hydrogels and results in a continuous 3D culture system that eliminates the need for subculturing.
- Over the course of the 6-week study, our 3D hydrogel system resulted in no significant changes in senescence, whereas traditional 2D culture resulted in an approximately fourfold increase in senescent ASC populations.
- Traditional 2D culture resulted in a significant decline in expression of stem-like MSC markers within one passaging event, and this continued to decline over the course of the study. Loss of expression of stem-like MSC markers was significantly slower in adipose-derived MSCs (ASCs) cultured within the 3D hydrogel system.
- Deterioration of the ASC phenotype over time in 2D correlated with a gradual decline in the regenerative capabilities for the ASC-conditioned medium, whereas the regenerative capabilities for the ASC-conditioned medium from 3D culture were sustained.

Supplementary data

To view the supplementary data that accompany this paper please visit the journal website at: www.futuremedicine.com/doi/suppl/10.2217/rme-2022-0140

Acknowledgments

Research reported in this publication was supported by KU startup funds (University of Kansas) and a MIRA grant from the National Institute of General Medical Sciences of the National Institutes of Health under award number R35GM143081. The content is solely the responsibility of the authors and does not necessarily represent the official views of the National Institutes of Health. Additional private commercial resources, including donation of the T-Block hydrogels, was provided by Ronawk. Lastly, the authors would like to acknowledge the team at Nikon for providing the fluorescent confocal images in Figure 1C & Supplementary Videos via their AXR Confocal Imaging System.

Financial & competing interests disclosure

Research reported in this publication was supported by KU startup funds (University of Kansas) and a MIRA grant from the National Institute of General Medical Sciences of the National Institutes of Health under Award Number R35GM143081. All authors declare that they do not have any conflict of interest except for A Mellott, who declares that they have financial interest with Ronawk, which is the company that produces and donated the T-Blocks used in this study. A Mellott is the co-founder and CEO of Ronawk. The authors have no other relevant affiliations or financial involvement with any organization or entity with a financial interest in or financial conflict with the subject matter or materials discussed in the manuscript apart from those disclosed.

No writing assistance was utilized in the production of this manuscript.

Open access

This work is licensed under the Attribution-NonCommercial-NoDerivatives 4.0 Unported License. To view a copy of this license, visit http://creativecommons.org/licenses/by-nc-nd/4.0/

References

Papers of special note have been highlighted as: • of interest

1. Hass R, Kasper C, Bohm S, Jacobs R. Different populations and sources of human mesenchymal stem cells (MSC): a comparison of adult and neonatal tissue-derived MSC. *Cell Commun. Signal.* 9, 12 (2011).

• **Review of mesenchymal stem/stromal cells (MSCs) and the different types of MSC populations, which also discusses the current and future role of MSC-derived regenerative therapies.**

2. Han Y, Li X, Zhang Y, Han Y, Chang F, Ding J. Mesenchymal stem cells for regenerative medicine. *Cells* 8(8), 886 (2019).
3. Pittenger MF, Discher DE, Peault BM, Phinney DG, Hare JM, Caplan AI. Mesenchymal stem cell perspective: cell biology to clinical progress. *NPJ Regen. Med.* 4, 22 (2019).
4. Musial-Wysocka A, Kot M, Majka M. The pros and cons of mesenchymal stem cell-based therapies. *Cell Transplant.* 28(7), 801–812 (2019).
5. Lukomska B, Stanaszek L, Zuba-Surma E, Legosz P, Sarzynska S, Drela K. Challenges and controversies in human mesenchymal stem cell therapy. *Stem Cells Int.* 2019, 9628536 (2019).
6. Koh J, Griffin DR, Archang MM *et al.* Enhanced *in vivo* delivery of stem cells using microporous annealed particle scaffolds. *Small* 15(39), e1903147 (2019).
7. Choe G, Park J, Park H, Lee JY. Hydrogel biomaterials for stem cell microencapsulation. *Polymers (Basel)* 10(9), 997 (2018).
8. Sivaraj D, Chen K, Chattopadhyay A *et al.* Hydrogel scaffolds to deliver cell therapies for wound healing. *Front. Bioeng. Biotechnol.* 9, 660145 (2021).
9. Trounson A, McDonald C. Stem cell therapies in clinical trials: progress and challenges. *Cell Stem Cell* 17(1), 11–22 (2015).
10. Walter MN, Wright KT, Fuller HR, Macneil S, Johnson WE. Mesenchymal stem cell-conditioned medium accelerates skin wound healing: an *in vitro* study of fibroblast and keratinocyte scratch assays. *Exp. Cell Res.* 316(7), 1271–1281 (2010).
11. Watson SL, Marcal H, Sarris M, Di Girolamo N, Coroneo MT, Wakefield D. The effect of mesenchymal stem cell conditioned media on corneal stromal fibroblast wound healing activities. *Br. J. Ophthalmol.* 94(8), 1067–1073 (2010).
12. Hu L, Wang J, Zhou X *et al.* Exosomes derived from human adipose mensenchymal stem cells accelerates cutaneous wound healing via optimizing the characteristics of fibroblasts. *Sci. Rep.* 6, 32993 (2016).
13. Eleuteri S, Fierabracci A. Insights into the secretome of mesenchymal stem cells and its potential applications. *Int. J. Mol. Sci.* 20(18), 4597 (2019).

14. Kabat M, Bobkov I, Kumar S, Grumet M. Trends in mesenchymal stem cell clinical trials 2004–2018: is efficacy optimal in a narrow dose range? *Stem Cells Transl. Med.* 9(1), 17–27 (2020).

15. Ahmed AS, Sheng MH, Wasnik S, Baylink DJ, Lau KW. Effect of aging on stem cells. *World J. Exp. Med.* 7(1), 1–10 (2017).

16. Jiang T, Xu G, Wang Q *et al. In vitro* expansion impaired the stemness of early passage mesenchymal stem cells for treatment of cartilage defects. *Cell Death Dis.* 8(6), e2851 (2017).

17. Yin Q, Xu N, Xu D *et al.* Comparison of senescence-related changes between three- and two-dimensional cultured adipose-derived mesenchymal stem cells. *Stem Cell Res. Ther.* 11(1), 226 (2020).

18. Drela K, Stanaszek L, Nowakowski A, Kuczynska Z, Lukomska B. Experimental strategies of mesenchymal stem cell propagation: adverse events and potential risk of functional changes. *Stem Cells Int.* 2019, 7012692 (2019).

- **Overview of current and ongoing limitations with MSC-derived therapies, with one major limitation being the non-standardized *ex vivo* expansion of MSCs that is needed for production of large-scale cell numbers and the adverse effects associated with this process.**

19. Izadpanah R, Kaushal D, Kriedt C *et al.* Long-term *in vitro* expansion alters the biology of adult mesenchymal stem cells. *Cancer Res.* 68(11), 4229–4238 (2008).

20. Baxter MA, Wynn RF, Jowitt SN, Wraith JE, Fairbairn LJ, Bellantuono I. Study of telomere length reveals rapid aging of human marrow stromal cells following *in vitro* expansion. *Stem Cells* 22(5), 675–682 (2004).

21. Engler AJ, Sen S, Sweeney HL, Discher DE. Matrix elasticity directs stem cell lineage specification. *Cell* 126(4), 677–689 (2006).

22. Dupont S. Role of YAP/TAZ in cell–matrix adhesion-mediated signalling and mechanotransduction. *Exp. Cell Res.* 343(1), 42–53 (2016).

23. Vining KH, Mooney DJ. Mechanical forces direct stem cell behaviour in development and regeneration. *Nat. Rev. Mol. Cell Biol.* 18(12), 728–742 (2017).

24. Ryu NE, Lee SH, Park H. Spheroid culture system methods and applications for mesenchymal stem cells. *Cells* 8(12), 1620 (2019).

25. Edmondson R, Broglie JJ, Adcock AF, Yang L. Three-dimensional cell culture systems and their applications in drug discovery and cell-based biosensors. *Assay Drug Dev. Technol.* 12(4), 207–218 (2014).

26. Zhou Y, Chen H, Li H, Wu Y. 3D culture increases pluripotent gene expression in mesenchymal stem cells through relaxation of cytoskeleton tension. *J. Cell. Mol. Med.* 21(6), 1073–1084 (2017).

- **Demonstrates the potential beneficial role of utilizing softer 3D culture substrates, such as hydrogels, for improving the retention/expression of pluripotent stem-like genes in MSC populations.**

27. Chaicharoenaudomrung N, Kunhorm P, Noisa P. Three-dimensional cell culture systems as an *in vitro* platform for cancer and stem cell modeling. *World J. Stem Cells* 11(12), 1065–1083 (2019).

28. Panchalingam KM, Jung S, Rosenberg L, Behie LA. Bioprocessing strategies for the large-scale production of human mesenchymal stem cells: a review. *Stem Cell Res. Ther.* 6, 225 (2015).

29. Kaminska A, Wedzinska A, Kot M, Sarnowska A. Effect of long-term 3D spheroid culture on WJ-MSC. *Cells* 10(4), 719 (2021).

30. Tibbitt MW, Anseth KS. Hydrogels as extracellular matrix mimics for 3D cell culture. *Biotechnol. Bioeng.* 103(4), 655–663 (2009).

31. Caliari SR, Burdick JA. A practical guide to hydrogels for cell culture. *Nat. Methods* 13(5), 405–414 (2016).

- **Excellent review describing the fabrication, utilization and benefits of 3D hydrogels for use in cell culture and cell therapies.**

32. Tsou YH, Khoneisser J, Huang PC, Xu X. Hydrogel as a bioactive material to regulate stem cell fate. *Bioact. Mater.* 1(1), 39–55 (2016).

33. Moshayedi P, Nih LR, Llorente IL *et al.* Systematic optimization of an engineered hydrogel allows for selective control of human neural stem cell survival and differentiation after transplantation in the stroke brain. *Biomaterials* 105, 145–155 (2016).

34. Chen J, Chin A, Almarza AJ, Taboas JM. Hydrogel to guide chondrogenesis versus osteogenesis of mesenchymal stem cells for fabrication of cartilaginous tissues. *Biomed. Mater.* 15(4), 045006 (2020).

35. Zigon-Branc S, Markovic M, Van Hoorick J *et al.* Impact of hydrogel stiffness on differentiation of human adipose-derived stem cell microspheroids. *Tissue Eng. A* 25(19–20), 1369–1380 (2019).

36. Bonab MM, Alimoghaddam K, Talebian F, Ghaffari SH, Ghavamzadeh A, Nikbin B. Aging of mesenchymal stem cell *in vitro*. *BMC Cell Biol.* 7, 14 (2006).

37. Chowdhury F, Li Y, Poh YC, Yokohama-Tamaki T, Wang N, Tanaka TS. Soft substrates promote homogeneous self-renewal of embryonic stem cells via downregulating cell-matrix tractions. *PLOS ONE* 5(12), e15655 (2010).

38. Gerardo H, Lima A, Carvalho J *et al.* Soft culture substrates favor stem-like cellular phenotype and facilitate reprogramming of human mesenchymal stem/stromal cells (hMSCs) through mechanotransduction. *Sci. Rep.* 9(1), 9086 (2019).

39. Wei W, Ma Y, Yao X *et al.* Advanced hydrogels for the repair of cartilage defects and regeneration. *Bioact. Mater.* 6(4), 998–1011 (2021).

40. Bai R, Tian L, Li Y *et al.* Combining ECM hydrogels of cardiac bioactivity with stem cells of high cardiomyogenic potential for myocardial repair. *Stem Cells Int.* 2019, 6708435 (2019).

41. Wang H, Shi J, Wang Y *et al.* Promotion of cardiac differentiation of brown adipose derived stem cells by chitosan hydrogel for repair after myocardial infarction. *Biomaterials* 35(13), 3986–3998 (2014).

42. Distler T, Lauria I, Detsch R *et al.* Neuronal differentiation from induced pluripotent stem cell-derived neurospheres by the application of oxidized alginate–gelatin–laminin hydrogels. *Biomedicines* 9(3), 261 (2021).

43. Burnsed OA, Schwartz Z, Marchand KO, Hyzy SL, Olivares-Navarrete R, Boyan BD. Hydrogels derived from cartilage matrices promote induction of human mesenchymal stem cell chondrogenic differentiation. *Acta Biomater.* 43, 139–149 (2016).

44. Han WM, Mohiuddin M, Anderson SE, Garcia AJ, Jang YC. Co-delivery of Wnt7a and muscle stem cells using synthetic bioadhesive hydrogel enhances murine muscle regeneration and cell migration during engraftment. *Acta Biomater.* 94, 243–252 (2019).

45. Dimmeler S, Leri A. Aging and disease as modifiers of efficacy of cell therapy. *Circ. Res.* 102(11), 1319–1330 (2008).

46. Schimke MM, Marozin S, Lepperdinger G. Patient-specific age: the other side of the coin in advanced mesenchymal stem cell therapy. *Front. Physiol.* 6, 362 (2015).

47. Rodier F, Campisi J. Four faces of cellular senescence. *J. Cell Biol.* 192(4), 547–556 (2011).

48. Van Deursen JM. The role of senescent cells in ageing. *Nature* 509(7501), 439–446 (2014).

49. Wagner W, Horn P, Castoldi M *et al.* Replicative senescence of mesenchymal stem cells: a continuous and organized process. *PLOS ONE* 3(5), e2213 (2008).

50. Acosta JC, Banito A, Wuestefeld T *et al.* A complex secretory program orchestrated by the inflammasome controls paracrine senescence. *Nat. Cell Biol.* 15(8), 978–990 (2013).

51. Turinetto V, Vitale E, Giachino C. Senescence in human mesenchymal stem cells: functional changes and implications in stem cell-based therapy. *Int. J. Mol. Sci.* 17(7), 1164 (2016).

52. Ratushnyy A, Ezdakova M, Buravkova L. Secretome of senescent adipose-derived mesenchymal stem cells negatively regulates angiogenesis. *Int. J. Mol. Sci.* 21(5), 1802 (2020).

- **One of many articles highlighting some of the negative effects of the secretome and paracrine signaling of MSC populations that have undergone senescence. The authors show how senescent MSC populations can impair angiogenesis.**

53. Liu J, Ding Y, Liu Z, Liang X. Senescence in Mesenchymal Stem Cells: Functional Alterations, Molecular Mechanisms, and Rejuvenation Strategies. *Front. Cell. Dev. Biol.* 8,258(2020).

54. Turinetto V, Vitale E, Giachino C. Senescence in Human Mesenchymal Stem Cells: Functional Changes and Implications in Stem Cell-Based Therapy. *Int. J. Mol. Sci.* 17(7), 1164 (2016).

55. Coppe JP, Desprez PY, Krtolica A, Campisi J. The senescence-associated secretory phenotype: the dark side of tumor suppression. *Annu. Rev. Pathol.* 5,99–118 (2010).